

Study of Bacterial Sensitivity to Ag-TiO₂ Nanoparticles

Tessy M. Lopez Goerne^{1,2,3*}, Mayra A. Alvarez Lemus², Verónica Angeles Morales⁴, Esteban Gómez López^{1,2} and Patricia Castillo Ocampo⁵

¹Health Department, Universidad Autónoma Metropolitana – Xochimilco, Mexico

²Nanotechnology Laboratory, National Institute of Neurology and Neurosurgery, Av. Insurgentes Sur 3877, Col. La Fama, Tlalpan, Mexico

³Department of Chemical and Biomolecular Engineering, Tulane University, New Orleans, LA 70118

⁴Infectology Department, National Institute of Neurology and Neurosurgery, Av. Insurgentes sur 3877, Col. La Fama, Tlalpan, México

⁵Laboratorio Central de Microscopia, División de Ciencias Básicas e Ingeniería Universidad Autónoma Metropolitana Iztapalapa, Mexico

Abstract

Background: Silver has been widely used for disinfection because of its well known antibacterial properties. Recently, silver nanoparticles have shown higher activity killing and inhibiting bacterial reproduction. In the present work we obtained silver nanoparticles highly dispersed over nanostructured titania in order to enhance bacterial sensitivity.

Materials and methods: Four different Titania-based nanoparticles were synthesized by the Sol-Gel process using Ag₂SO₄, AgCl, AgNO₃ and CH₃COOAg as silver precursor. All the materials were characterized by FTIR, UV-Vis and XPS, TEM microscopy, EDS, also BET and DRX analysis were carried out.

Results: Amorphous materials were apparently obtained. Ag-TiO₂ nanoparticles were tested against several Gram-negative and Gram-positive bacteria including enteropathogenic *Escherichia coli* and highly resistant strains such as methicillin-resistant *Staphylococcus aureus* and they showed sensibility in most of cases.

Conclusions: Supported silver nanoparticles represent a suitable way to obtain highly dispersed active silver over higher surface area. This approach allows its use as efficient bactericide since lower silver amount can be employed.

Keywords: Nanosilver; Nanostructured titania; Sol-gel; Bactericide; *Staphylococcus aureus*

Introduction

Nanotechnology has become one of the most explored fields in the last decade [1-3]. Due to the possibility to manipulate matter at atomic level, nanotechnology allows to control specific properties to obtain novel materials. Materials which size is reduced to the nanoscale often exhibit new and unique properties, interesting for academy and useful from technological perspective. Technological advances in the field of imaging at this level have allowed new insight and new mechanistic understanding.

Most of the reports on Nanotechnology include environmental care and human health. Diagnosis and treatment are the main focus of these novel technologies. In this sense, despite of all the efforts, hospital acquired infections still remain among the main leading causes of death all over the world. Nosocomial infection represents a serious problem worldwide, because of treatment increases hospital costs significantly. According to a study implemented by (World Health Organization) WHO, 55 hospitals of 14 different countries, showed that 8.7% of hospitalized patients had nosocomial infections (WHO/CDS/CSR/EPH/2002.12). Bacterial resistance against antimicrobial agents is a phenomenon characterized by partial or total refractoriness of microorganisms, for example *Staphylococcus aureus* has developed resistance to penicillin and methicillin. This is an acquired resistance, where bacterial DNA mutates. Bactericides are an important example of nanobiotechnology applications.

It is well known that nanomaterials can interact with cells and bacteria [4,5]. Morphology and topography as well as their surface physics and chemistry strongly influences the way microorganisms respond to nanostructures [6] and these properties depend on the obtaining process.

Silver solutions and silver supported materials have been widely used as bactericide and fungicide [7-9]. Silver nanoparticles in solution or supported on appropriate substrates are currently used due to their

effective action affecting the cellular metabolism and inhibiting cell growth [10]. The chemistry has revealed that silver deposits are non toxic for human cells in vivo and is also reported as a biocompatible material [11-13].

Colloidal and silver salts have several limitations due to the cost of Ag and their toxicity at high concentrations. Nevertheless, supported silver particles obtained by the sol-gel process are a successful technology when fixed on adequate supports due to their increased bactericide effect [14]. Besides well dispersion of silver, high contact surface is necessary to increase the bactericide effect. The preparation of uniform nanosized particles with specific requirements of size, shape, and physico-chemical properties are of great interest in the formulation of new products with many biotechnological applications [15,16].

Resistance of bacteria to bactericides and antibiotics has increased in recent years due to the progress of resistant strains. Some antimicrobial agents are extremely irritant and toxic and current researches are focused on formulate new types of safe and cost-effective biocide materials.

On the other hand, nano structured reservoirs made of inorganic oxides like TiO₂, and synthesized by the sol-gel process, have been demonstrated to be biocompatible and suitable supports for a wide variety of compounds [17].

*Corresponding author: Tessy M. Lopez Goerne, Health Department, Universidad Autónoma Metropolitana – Xochimilco, Calzada del Hueso 1100, Col. Villa Quietud, Delegación Coyoacán, C. P. 04960, D.F. México, E-mail: tessy3@prodigy.net.mx

Received March 30, 2012; Accepted May 21, 2012; Published May 25, 2012

Citation: Lopez Goerne TM, Alvarez Lemus MA, Morales VA, López EG, Ocampo PC (2012) Study of Bacterial Sensitivity to Ag-TiO₂ Nanoparticles. J Nanomed Nanotechnol S5:003. doi:10.4172/2157-7439.S5-003

Copyright: © 2012 Lopez Goerne TM, et al. This is an open-access article distributed under the terms of the Creative Commons Attribution License, which permits unrestricted use, distribution, and reproduction in any medium, provided the original author and source are credited.

The size-dependent Ag/TiO₂ interaction of silver nanoparticles with gram-negative bacteria and virus has also been showed [18-20]. The electrostatic attraction between negatively charged bacterial cells and positively charged nanoparticles is fundamental for its activity as bactericide [21,22].

Morones et al. [23] reported that PVC interacts with titania and can be used as bactericide. The material can be modified in order to improve its behavior against bacteria, for this reason it is important the use of nanoparticles with a high surface area and a well dispersion of the silver particles on the support that increases the contact interface between the bactericidal (silver) and bacteria [24-28].

Since TiO₂ has photocatalytic properties [29], some researchers have also used these basics together with the silver antibacterial properties to prepare silver supported titania materials as a photocatalytic bactericide [30-32].

In the present work, we prepared silver nanoparticles supported on titania sol-gel method using different silver precursors. Antibacterial behavior of the nanomaterials was tested with different bacterial cultures by making the disk susceptibility tests. In order to study and correlate antibacterial activity and physicochemical properties of the materials as well as the effect of the precursor, FTIR and UV-Vis spectroscopies, BET and XRD characterization was carried out.

Materials and Methods

Ag/TiO₂ nanoparticles synthesis

Ag/TiO₂ nanomaterials were prepared by the sol-gel method using titanium n-butoxide (Sigma, 98.5%), ethanol, water and the corresponding amount of silver precursor (10% wt Ag). Silver precursors used were silver acetate (CH₃COOAg) (Sigma, 99%), silver nitrate (AgNO₃) (Sigma, 99%), silver chloride (AgCl) (Sigma, 99.999%) and silver sulfate (Ag₂SO₄, Sigma, 99.99%). Ammonium hydroxide (NH₄OH, J.T. Baker, 28-30%) was used to adjust the pH to 9.

Characterization

XRD studies were made using Cu K α radiation, in Siemens D-500 equipment. The signal intensity was measured by step scanning in the 2 θ range with a step of 0.03° and a measuring time of 2s per point.

Infrared spectra were collected in a Perkin Elmer's Spectrophotometer, 32 scans. The powder samples were mixed with KBr and pressed into a disk.

Surface areas of the samples were measured on a Micromeritic ASAP 2010 Quantasorb Sorptometer and calculated by the nitrogen isotherms using the BET method. The mean pore diameter was calculated by the BJH method.

UV-Vis analysis was carried out in a Cary 1 Varian spectrophotometer with integration sphere, sample powders were measured without making previous treatment.

The powder samples were analyzed by conventional transmission electron microscopy (TEM) in order to determine the particle size, these analysis were performed on a Zeiss EM910 electron microscope operated at 100 kV, with a 0.4 nm point to point resolution side entry goniometer attached to a CCD Mega Vision III image processor.

X-ray Photoelectron Spectra (XPS) were acquired with a VG-Microtech Multilab 3000 spectrometer equipped with a hemispherical electron analyzer and a Mg K α (h = 1253.6 eV, 1 eV = 1.6302 \times 10⁻¹⁹ J)

300-W X-ray source. The powder samples were pressed into small Inox cylinders and then mounted on a sample rod placed in a pre-treatment chamber. Before recording the spectrum, the sample was maintained in the analysis chamber until a residual pressure of ca. 4 \times 10⁻⁹ Torr was reached. Spectra were collected at pass energy of 50 eV. The intensities were estimated by calculating the integral of each peak, after subtraction of the S-shaped background, and by fitting the experimental curve to a combination of Lorentzian (30%) and Gaussian (70%) lines. All Binding Energies (B.E.) were referenced to the C 1s line at 284.6 eV, which provided binding energy values with an accuracy of \pm 0.2 eV.

Bacterial strains

Pseudomona aeruginosa, *Klebsiella pneumoniae*, *Serratia marcescens*, *Proteus vulgaris*, enteropathogenic *Escherichia coli* (EPEC), *Salmonella typhimurium*, *Shigella dysenteriae*, from collection of our laboratory; *Staphylococcus aureus* (ATCC 25923), and methicillin-resistant *Staphylococcus aureus* (MRSA) (ATCC 43300), were used.

Bacterial sensibility test

To examine the susceptibility of bacterial strains to silver nanoparticles, a Kirby-Bauer disk-diffusion method was used, following the recommended criteria of CLSI (12). Disks of Whatman filter paper (7mm) were soaked with a 0.1% solution of samples labeled Ag-NO₃-TiO₂-, Ag-SO₄-TiO₂, Ag-Cl-TiO₂ and Ag-Ac-TiO₂. Bacterial strains were spread onto Mueller-Hinton agar with cotton swabs from freshly grown bacterial suspension (0.5 McFarland densities). The inoculated agar plates were allowed to dry and then the round disks with Ag-nanoparticles were placed on top of the inoculated agar. The agar plates were incubated at 37°C for 18h. The diameter of the zone of inhibition was measured using a caliper. The experiments were performed on triplicate to obtain average values for each strain.

Results

It has been extensively reported the introduction of metals ions, into metal oxides like TiO₂ in order to enhance its catalytic or photocatalytic properties [33,34]. The foreign metal ions, usually affect the TiO₂ phase transformation behavior and structure when they are introduced by sol-gel method [35].

Diffraction patterns of the samples are shown in Figure 1. All samples, silver acetate, sulfate, nitrate and chloride supported on nanostructured titania, showed an amorphous pattern. No signal at 25.281 (2 θ) neither

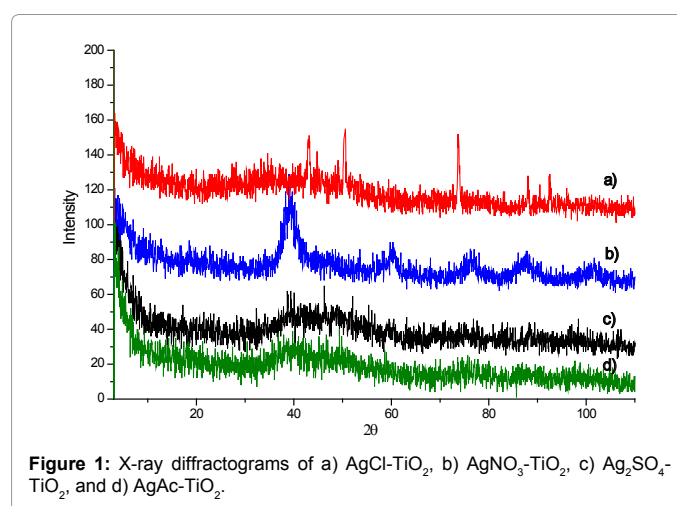


Figure 1: X-ray diffractograms of a) AgCl-TiO₂, b) AgNO₃-TiO₂, c) Ag₂SO₄-TiO₂, and d) AgAc-TiO₂.

27.44 (2θ) for anatase (1 0 1) or rutile (1 1 0) were observable. No peaks related to Ag were observed in the samples except in AgNO₃-TiO₂ sample. Those peaks at 39.3(2θ) and 60.3(2θ) showed in AgNO₃-TiO₂ sample can be attributed to the presence of Ag metal when silver nitrate is used as precursor [36].

FTIR spectra are shown in Figure 2. The bands observed in the high energy region of the spectra at 3390, 3399, 3401 and 3411 cm⁻¹ for all the samples and are associated with the presence of hydroxyl groups. The bands at 1623, 1627, 1629 cm⁻¹, are related to the presence of C-H vibrations and 1633 cm⁻¹ is assigned to the bending frequency O-H bond in water; whereas the band located at 1384 cm⁻¹ corresponds to a vibration of the Ti-Ligand bond. In sulfate salt sample, we observed a decrease in the intensity of the band at 1384 cm⁻¹ and the presence of two bands in 1135 and 1051 cm⁻¹ related to the sulfate anion bonding to the surface. For the acetate salt we can see a band at 1536 related to the C=O group of the acetate. For sulfate salt we have an important result because the FTIR results indicate a sulfated titania with high acidity and a great stability. Instead of this we have a helpful aspect of the sulfated titania, which has been reported to be a solid acid [37,38].

UV-Vis spectra (Figure 3) were collected for all the samples. The band gap (E_g) values of the samples were calculated resulting almost constant in all nanomaterials (Table 1). Characteristic absorption band from titania was observed at 330 nm, indicating the presence of titanium dioxide. A weak overlapped shoulder around 430 nm in the AgAc-TiO₂ material. Visible absorption for the rest nanomaterials is related with the presence of silver oxide, due to change in color from white (pure TiO₂) to gray.

Figure 4 shows N₂ adsorption isotherms and pore size distribution (inset). All the materials showed a type IV isotherm (IUPAC) [39] characteristic of mesoporous materials. The hysteresis loop of the sample AgCl-TiO₂ corresponds to a type H1, associated with porous materials that consist of agglomerates or compacts of approximately uniform spheres in fairly regular array. For the rest of the samples we observed a type H4 associated with narrow slit-like pores. Surface area and mean pore diameter are reported in Table 2.

Figure 5 shows TEM images of Ag-TiO₂ samples, particle size is in the range of 5-10 nm in all the samples. Ag₂SO₄-TiO₂ and AgNO₃-TiO₂ showed a uniform distribution and similar morphologies with semi-spherical aggregates, this may be due to the similarity between the ions. In Ag₂SO₄-TiO₂ micrograph (Figure 6) some regions where the crystalline structures are observable, have been chosen (red lines). However, there are zones with apparently non-organized structure. Elemental analysis of this sample is showed in Figure 7.

In order to elucidate what type of Ag chemical species are present on the materials, XPS study was performed. In Figure 8, O1s spectra for all the samples are shown. We observed three different oxygen species in acetate and nitrate samples. In silver acetate-titania sample the first peak appears at 528.2 eV, the BE low value for oxygen signal has been reported to oxygen bonded to metals in polyhedral coordination, the second one appears at 529.8 eV and corresponds to oxide, and is in agreement to those values reported for TiO₂ materials [40] this signal is centered at 529.68 for silver nitrate nanomaterial. Finally, the peak at 531.7 [41] is associated to OH groups from adsorbed water and surface hydroxylation. In AgNO₃-TiO₂ the highest value at 533.6 eV is related with the presence of C=O or C-O due to ethanol. For AgCl and Ag₂SO₄ samples only the corresponding signals from oxide

and hydroxyl groups were observed. The highest intensity of OH corresponding oxygen signal was in AgNO₃-TiO₂ and is in agreement

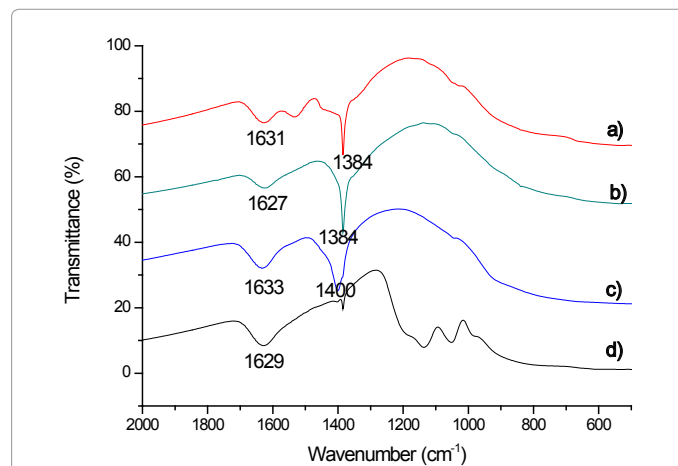


Figure 2: FTIR spectra of nanostructured a) AgAc-TiO₂, b) AgNO₃-TiO₂, c) AgCl-TiO₂ and d) Ag₂SO₄-TiO₂ samples.

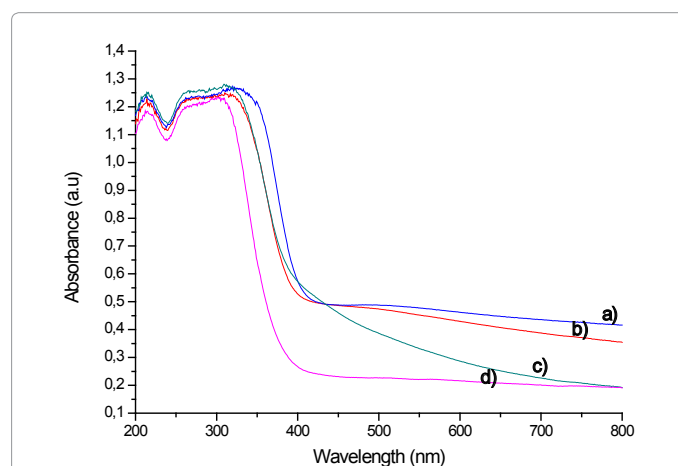


Figure 3: UV-Vis spectra of a) AgNO₃-TiO₂, b) Ag₂SO₄-TiO₂, c) AgAc-TiO₂ and d) AgCl-TiO₂.

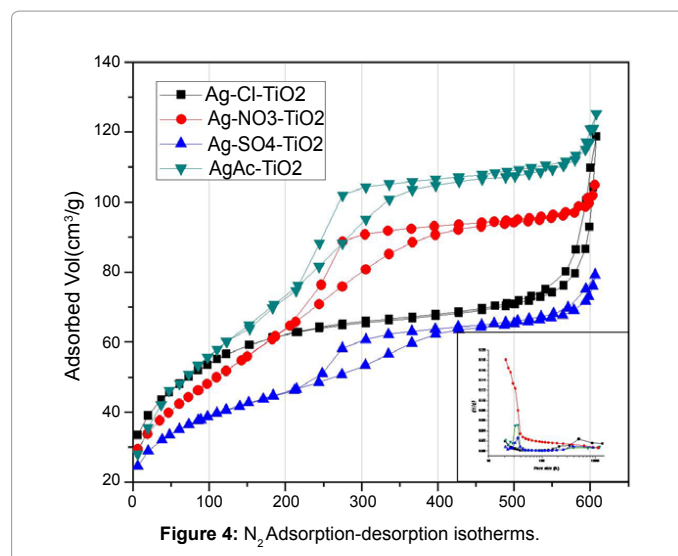


Figure 4: N₂ Adsorption-desorption isotherms.

with the observed by (Fourier Transform Infrared Spectroscopy) FTIR in the high energy region.

In the Ti 2p spectra a Ti 2p_{1/2} peak was presented at 464.4 eV in all samples, which is characteristic of Ti⁴⁺ [42]. Slitting between 2p_{3/2} and 2p_{1/2} core levels are 6 eV for most of the samples and 5.9 eV for Ag₂SO₄-TiO₂. In this nanomaterial, a slight shift to higher energy in both signals was observed (459.18 and 465.08 eV respectively), which is associated to the presence of Ti³⁺ species. Also, in AgAc-TiO₂ two small shoulders at 457.28 and 463.28 eV corresponding to Ti³⁺ was detected [43]. Ag 3d spectra showed the presence of Ag⁰ and Ag⁺ species in AgAc-TiO₂, AgCl-TiO₂ and AgNO₃-TiO₂ nanomaterials, and probably another coordinated Agⁿ⁺ species in AgNO₃-TiO₂ and Ag₂SO₄-TiO₂ samples (Table 3).

Sample	Eg value (eV)
TiO ₂ -Cl-Ag	3.18
TiO ₂ -SO ₄ -Ag	2.86
TiO ₂ -Ac-Ag	2.86
TiO ₂ -NO ₃ -Ag	2.84

Table 1: Eg values calculated from the UV-Vis spectra.

Sample	BET surface area (m ² /g)	Mean pore diameter (Å)
TiO ₂ -NO ₃ -Ag	192	33
TiO ₂ -Ac-Ag	228	33
TiO ₂ -SO ₄ -Ag	143	33
TiO ₂ -Cl-Ag	200	32

Table 2: BET surface areas and BJH mean pore diameter.

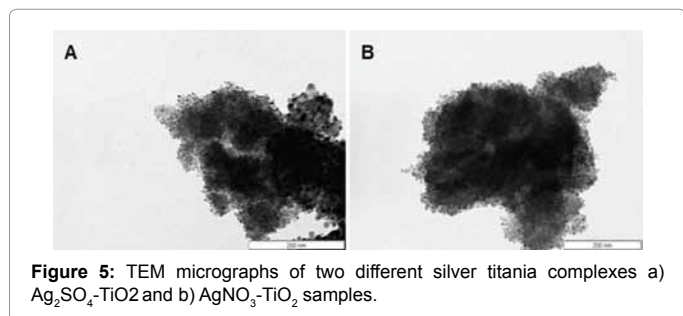


Figure 5: TEM micrographs of two different silver titania complexes a) Ag₂SO₄-TiO₂ and b) AgNO₃-TiO₂ samples.

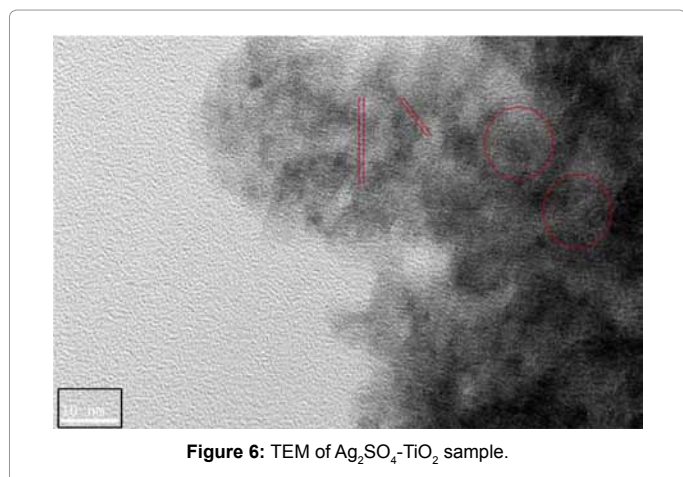


Figure 6: TEM of Ag₂SO₄-TiO₂ sample.

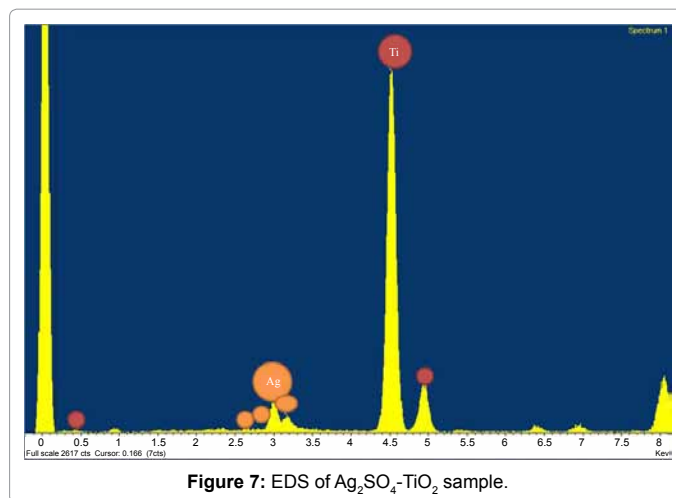


Figure 7: EDS of Ag₂SO₄-TiO₂ sample.

Antibacterial and Antifungal Properties of Ag-Nanoparticles

The antibacterial and antifungal properties of silver nanoparticles were evaluated using the disk diffusion test. The filter paper disks with Ag nanoparticles placed on the bacteria or fungus-inoculated agar plates killed the bacteria or fungus under and around them; we observed different zones of growth inhibition around the disk depending on microorganism strain and Ag-nanoparticles. The zones of inhibition for disks of 0.1% Ag-nanoparticles solutions are given in Table 4. The major inhibition effect was presented by AgSO₄, followed by AgAc and AgNO₃, and finally AgCl with the minor inhibition (Figure 9 and Figure 10). Using TiO₂ alone, no considerable inhibition effect was observed, only a poor inhibition in *K. pneumoniae* and *S. marcescens* was detected (Table 2). All the bacterial strains and *C. albicans* were inhibited by the nanoparticles, except *P. vulgaris* with a poor inhibition. All the bacterial strains and *C. albicans* were inhibited by nanoparticles except *P. vulgaris* with a poor inhibition. MSSA was inhibited better with all the nanoparticles.

Discussion

Silver nanoparticles over titania has been demonstrated its antibacterial properties [44], their reactivity strongly depend on synthesis method. Sol-gel process provides an excellent alternative since many parameters can be controlled. Addition of agents during gelation step give enhanced properties to obtained powders. Moreover, an additional parameter has been considered in recent studies: silver ions release, since sol-gel allow to incorporate foreign atoms into its lattice when are added at the beginning of the process, one can obtain several advantages like point defects due to oxygen vacancies, and strong interactions between foreign metal and support. In this work we obtained the Ag-TiO₂ materials by adding “in situ” the corresponding silver compound. By this procedure, we optimize and facilitate strong metal-support interactions, and thus release or delivery of silver-silver ions diminishes compared with other obtaining methods like impregnation. Although all the samples were apparently amorphous, it is well known that some materials can exhibit nano-crystallinity; in our case this phenomenon was presented by Ag₂SO₄ sample as some areas where small crystals are clearly observed. That is the reason why is undetectable by conventional X-Ray. In the other hand, interactions between metal and support are related with the chemical nature of silver precursor. For AgAc-TiO₂ nanomaterial, we can assume the presence

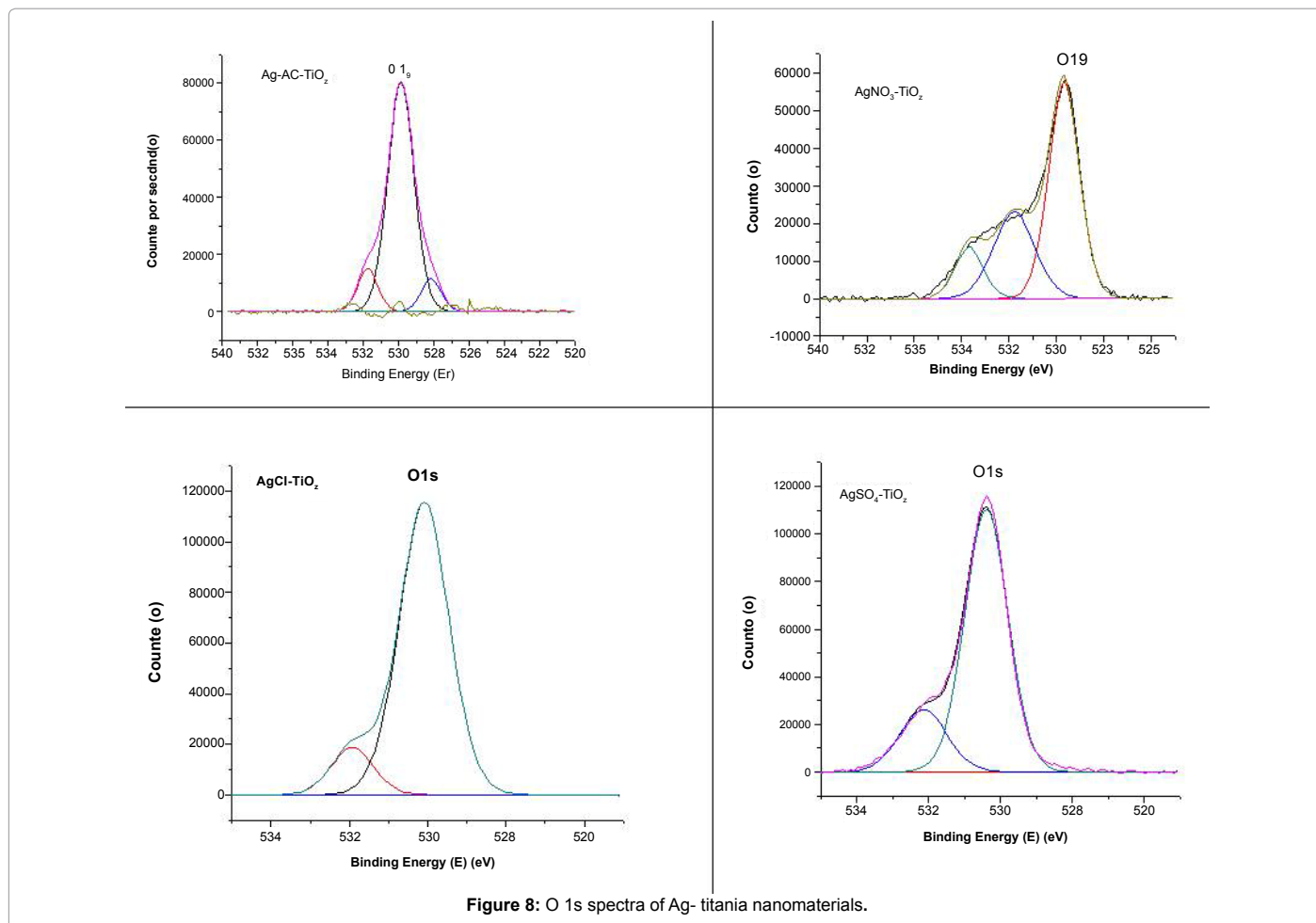


Figure 8: O 1s spectra of Ag- titania nanomaterials.

Sample	%Ag total amount	BE (eV)	% Ag ⁺	BE (eV)	% Ag	BE (eV)	% Ag ⁿ
AgAc	2.82	366.5	0.57	368	2.25	-	-
AgCl	1.04	366.8	0.55	368	0.49	-	-
AgNO ₃	4.69	367.5	3.81	368.5	0.63	371	0.25
AgSO ₄	2.39	-	-	368	2.26	369.5	0.13

Table 3: Silver species and percentage calculated by XPS.

Microorganism	Zone of inhibition (mm) ^a				
	TiO ₂ -NO ₃ -Ag	TiO ₂ -Cl-Ag	TiO ₂ -Ac-Ag	TiO ₂ -SO ₄ -Ag	TiO ₂
<i>Pseudomonas aeruginosa</i>	11	10	11.3	11	-
<i>Salmonella typhimurium</i>	9	9	8.1	9.7	-
<i>Proteus vulgaris</i>	7.2	7.2	7.2	-	-
<i>Klebsiella pneumoniae</i>	10	8.7	9	9	7.7
<i>E. coli</i> (EPEC)	10	9.3	10	9.3	-
<i>Shigella dysenteriae</i>	10	10.5	10.7	10.7	-
<i>Serratia marcescens</i>	10	9	9.3	10.3	8
<i>Staphylococcus aureus</i> (MRSA)	10.3	10	10.7	10.7	-
<i>Staphylococcus aureus</i> (MSSA)	15.3	14.5	15	14	-
<i>Candida albicans</i>	10	8.7	9.3	10.3	-

^aDisk's diameter was 7 mm

Table 4: Zone of inhibition with the Ag-nanoparticles.

of silver nanoparticles, these could be obtained by reduction induced by OH groups from synthesis method, and is confirmed by XPS analysis. Ti³⁺ is considered to be an important reactive agent; hence many surface reactions are influenced by these point defects. Sol-gel method

is an excellent procedure to obtain these types of defects. In AgAc-TiO₂ sample as well as Ag₂SO₄-TiO₂ Ti³⁺ defects are present, giving some special reactivity toward bacteria surface over AgCl-TiO₂. Supported Ag-nanoparticles have bactericide effect over Gram negative and Gram

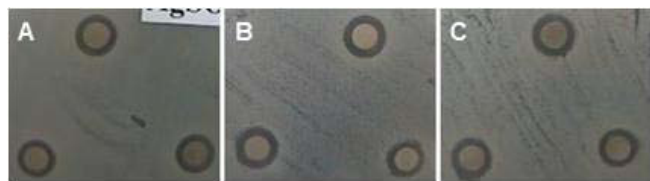


Figure 9: Disk diffusion test, zone of growth inhibition: A) *Pseudomonas aeruginosa* with AgAc-TiO₂; B) *Klebsiella pneumoniae* with AgNO₃; C) *E. coli* EPEC with Ag₂NO₃.



Figure 10: Disk diffusion test, zone of growth inhibition: A) *Staphylococcus aureus* (MSSA) with Ag₂SO₄-TiO₂; B) *Staphylococcus aureus* (MSSA) with AgAc-TiO₂; C) *Staphylococcus aureus* (MSSA) with AgNO₃-TiO₂.

positive bacteria, which make them a broad spectrum bactericide. The major effect was observed with AgNO₃ precursor, this can be explained by the presence of metallic silver dispersed on titania surface and the presence of nitrate. A common feature is the high surface area values of the samples, although TiO₂-Ac-Ag showed the highest, acetate group is a strong ligand that can interact with TiO₂ inhibiting the Ag activity. Two of all the bacteria's used *E. coli* enteropatogénica and *S. aureus*, have a high grade of pathogenicity, and also they are methicillin resistant. Both were destroyed by all Ag-nanoparticles, being the less active TiO₂-Cl-Ag, this can be related to capability of chlorine ions to neutralize titania surface charge.

Conclusion

The increase of bacterial resistance to antimicrobial agents is a serious problem in the treatment of infectious diseases as well as in epidemiological survey. Progressively more new bacterial strains have emerged with dangerous levels of resistance, including both Gram-positive and Gram-negative bacteria. The bacterial resistance will require precautions that guide to prevention of the emergence and spreading of multi resistance bacterial strains, and the development of new antimicrobial substance. The results of this study demonstrated that nanostructured sol-gel TiO₂-Ag have a bactericide effect including highly pathogenic bacteria such as EPEC and MRSA even more than conventional bactericides with the advantage of suitability for repeated use with potential to surface application. Additionally, obtained results on Eg values as well as parameters like OH groups quantification suggest the possibility to use these composites as photocatalysts against bacteria.

Acknowledgements

We would like to thank to CONACyT-FONCICYT 96095 project, UAM for financial support and INNN-Neuro infectology Department. Also thank to J. Bustos, L. Albarran and P. Quintana for technical assistance. Specially thanks to Dr. Francisco Rodriguez Reinoso and Dra. Ana Silvestre Albero for XPS analysis.

References

1. Koo OM, Rubinstein I, Onyukel H (2005) Role of nanotechnology in targeted drug delivery and imaging: a concise review. *Nanomedicine* 1: 193-212.

2. Sahoo SK, Parveen S, Panda JJ (2007) The present and future of nanotechnology in human health care. *Nanomedicine* 3: 20-31.

3. Corbett J, McKeown PA, Peggs GN, Whatmore R (2000) Nanotechnology: international development and emerging products. *CIRP Annals - Manufacturing Technology* 49: 523-545.

4. Nguyen CA, Allémann E, Schwach G, Doelker E, Gurny R (2003) Cell interaction studies of PLA-MePEG nanoparticles. *Int J Pharm* 254: 69-72.

5. García A, Delgado L, Torà JA, Casals E, González E, et al. (2012) Effect of cerium dioxide, titanium dioxide, silver, and gold nanoparticles on the activity of microbial communities intended in wastewater treatment. *J Hazard Mater* 199-200: 64-72.

6. Anselme K, Davidson P, Popa AM, Giazzon M, Liley M, et al. (2010) The interaction of cells and bacteria with surfaces structured at the nanometre scale. *Acta Biomater* 6: 3824-3846.

7. Ershov G, Janata E, Henglein A (1993) Growth of silver particles in aqueous solution: long-lived "magic" clusters and ionic strength effects *J Phys Chem* 97: 339-343.

8. Fu-Ren F, Bard AJ (2002) Chemical, Electrochemical, Gravimetric, and Microscopic Studies on Antimicrobial Silver Films. *J Phys Chem* 106: 279-287.

9. Zhao G, Stevens SE Jr (1998) Multiple parameters for the comprehensive evaluation of the susceptibility of *Escherichia coli* to the silver ion. *Biomaterials* 11: 27-32.

10. Akhavan O, Ghaderi E (2009) Capping antibacterial Ag nanorods aligned on Ti interlayer by mesoporous TiO₂ layer. *Surf Coat Technol* 203: 3123-3128.

11. Tilton RC, Rosenberg B (1978) Reversal of the silver inhibition of microorganisms by agar. *Appl Environ Microbiol* 35: 1116-1120.

12. Naoi K, Ohko Y, Tatsuma T (2004) TiO₂ Films Loaded with Silver Nanoparticles: Control of Multicolor Photochromic Behavior. *J Am Chem Soc* 126: 3664-3668.

13. Kusnetsov J, Iivanainen E, Elomaa N, Zacheus O, Martikainen PJ (2001) Copper and silver ions more effective against *Legionellae* than against mycobacteria in a hospital warm water system. *Water Res* 35: 4217-4225.

14. Magaña SM, Quintana P, Aguilar DH, Toledo JA, Angeles-Chávez MA, et al. (2008) Antibacterial activity of montmorillonites modified with silver. *J Mol Catal A Chem* 281: 192-199.

15. Lopez T, Navarrete J, Conde R, Ascencio JA, Manjarrez J, et al. (2006) Molecular vibrational analysis and MAS-NMR spectroscopy study of epilepsy drugs encapsulated in TiO₂-sol-gel reservoirs. *J Biomed Mater Res A* 78: 441-448.

16. Mena-Duran CJ, Sun Kou MR, Lopez T, Azamar-Barrios JA, Aguilar DH, et al. (2007) Nitrate removal using natural clays modified by acid thermoactivation. *Appl Surf Sci* 253: 5762-5766.

17. Peterson A, Lopez T, Ortiz-Islas E, González RD (2007) Pore structures in an implantable sol-gel titania ceramic device used in controlled drug release applications: A modeling study. *Appl Surf Sci* 253: 5767-5771.

18. Lee D, Cohen RE, Rubner MF (2005) Antibacterial Properties of Ag Nanoparticle Loaded Multilayers and Formation of Magnetically Directed Antibacterial Microparticles. *Langmuir* 21: 9651-9659.

19. Li P, Li J, Wu C, Wu Q, Li J (2005) Synergistic antibacterial effects of β -lactam antibiotic combined with silver nanoparticles. *Nanotechnol* 16: 1912.

20. Guzman M, Dille J, Godet S (2012) Synthesis and antibacterial activity of silver nanoparticles against gram-positive and gram-negative bacteria. *Nanomed Nanotechnol Biol Med* 8: 37-45.

21. Stoimenov PK, Klinger RL, Marchin GL, Klabunde KJ (2002) Metal Oxide Nanoparticles as Bactericidal Agents. *Langmuir* 18: 6679-6686.

22. Hamouda T, Baker Jr JR (2000) Antimicrobial mechanism of action of surfactant lipid preparations in enteric Gram-negative bacilli. *J Appl Microbiol* 89: 397-403.

23. Morones JR, Elechiguerra JL, Camacho A, Holt K, Kouri JB, et al. (2005) The bactericidal effect of silver nanoparticles. *Nanotechnology* 16: 2346.

24. Elechiguerra JL, Burt JL, Morones JR, Camacho-Bragado A, Gao X, et al. (2005) Interaction of silver nanoparticles with HIV-1. *J Nanobiotechnology* 3: 6.

25. Evans P, Sheel DW (2007) Photoactive and antibacterial TiO₂ thin films on stainless steel. Surf Coat Technol 201: 9319-9324.
26. Tseng I, Wu JC (2004) Chemical states of metal-loaded titania in the photoreduction of CO₂. Catal Today 97: 113-119.
27. Gómez R, López T, Ortiz-Islas E, Navarrete J, Sánchez E, et al. (2003) Effect of sulfation on the photoactivity of TiO₂ sol-gel derived catalysts. J Mol Catal A Chem 193: 217-226.
28. Yuranova T, Rincon AG, Pulgarin C, Laub D, Xantopoulos N, et al. (2006) Performance and characterization of Ag-cotton and Ag/TiO₂ loaded textiles during the abatement of E. coli. J Photochem Photobiol A Chem 181: 363-369.
29. Chun H, Yuchao T, Hongxiao T (2005) Characterization and photocatalytic activity of transition-metal-supported surface bond-conjugated TiO₂/SiO₂. Catal Today 90: 325-330.
30. Castro L, Reyes P, de Correa CM (2002) Synthesis and Characterization of Sol-Gel Cu-ZrO₂ and Fe-ZrO₂ Catalysts. J Sol-Gel Sci Technol 25: 159-168.
31. Chao HE, Yun YU, Xingfang HU, Larbot A (2003) Effect of silver doping on the phase transformation and grain growth of sol-gel titania powder. J Eur Ceram Soc 23: 1457-1464.
32. Akhavan O (2009) Lasting antibacterial activities of Ag-TiO₂/Ag/a-TiO₂ nanocomposite thin film photocatalysts under solar light irradiation. J Colloids Interface Sci 336: 117-124.
33. Amin SA, Pazouki M, Hosseinnia A (2009) Synthesis of TiO₂-Ag nanocomposite with sol-gel method and investigation of its antibacterial activity against E. coli. Powder Technol 196: 241-245.
34. Pal S, Tak YK, Song JM (2007) Does the Antibacterial Activity of Silver Nanoparticles Depend on the Shape of the Nanoparticle? A Study of the Gram-Negative Bacterium *Escherichia coli*. Appl Environ Microbiol 73: 1712-1720.
35. Hamouda T, Hayes MM, Cao Z, Tonda R, Johnson K, et al. (1999) A Novel Surfactant Nanoemulsion with Broad-Spectrum Sporicidal Activity against *Bacillus* Species. J Infect Dis 180: 1939-1949.
36. Chai L, Wei S, Peng B, Li Z (2008) Effect of thermal treating temperature on characteristics of silver-doped titania. Trans Nonferrous Met Soc China 18: 980-985.
37. Baylet A, Capdeillayre C, Retailleau L, Vernoux P, Figueras F, et al. (2010) Relation between partial propene oxidation, sulphate content and selective catalytic reduction of NOx by propene on ceria/sulphated titania. Appl Catal B 96: 434-440.
38. Holbrook BM, Baylet A, Retailleau L, Boreave A, Vernoux P, et al. (2011) Sulphated TiO₂ for selective catalytic reduction of NOx by n-decane. Catal Today 176: 48-55.
39. Sing KSW (1982) Reporting physisorption data for gas/solid systems with special reference to the determination of surface area and porosity. Pure & Appl Chem 54: 2201-2218.
40. Leinen D, Fernandez A, Espinos JP, Holgado JP, González-Elipe AR (1993) An XPS study of the mixing effects induced by ion bombardment in composite oxides. Appl Surf Sci 68: 453-459.
41. Lim AS, Atrens A (1990) ESCA studies of nitrogen-containing stainless steels. Applied Physics A Solids and Surfaces 51: 411-418.
42. Shao G, Liu L, Ma T, Wang F, Ren T, et al. (2010) Synthesis and characterization of carbon-modified titania photocatalysts with a hierarchical meso-/macroporous structure. Chem Eng J 160: 370-377.
43. Xiong L, Li J, Yang B, Yu Y (2012) Ti³⁺ in the Surface of Titanium Dioxide: Generation, Properties and Photocatalytic Application. J Nanomater.
44. Liu Y, Wang X, Yang F, Yang X (2008) Excellent antimicrobial properties of mesoporous anatase TiO₂ and Ag/TiO₂ composite films. Microporous Mesoporous Mater 114: 431-439.

This article was originally published in a special issue, **Nanotechnology: Challenges & Perspectives in Medicine** handled by Editor(s) Dr. Malavosklish Bikram, University of Houston, USA